

# FERRITE HARDNESS INCREASES DUE TO STRUCTURAL CHANGES AT LOW TEMPERATURES IN DUPLEX STAINLESS STEELS

**João Roberto Sartori Moreno<sup>1</sup>, joaosartori@utfpr.edu.br**

UTFPR – Universidade Tecnológica Federal do Paraná – Av. Alberto Carazzai, 1640 Cornélio Procópio – PR -86300-000

**Fabiano Moreno Peres<sup>2</sup>, fabianoperes@utfpr.edu.br**

UTFPR – Universidade Tecnológica Federal do Paraná – Av. dos Pioneiros, 3131 Londrina – PR - 86036-370

**Luiz Carlos Cegatti do Nascimento<sup>3</sup>, cegatti@utfpr.edu.br**

UTFPR – Universidade Tecnológica Federal do Paraná – Av. Alberto Carazzai, 1640 Cornélio Procópio – PR -86300-000

**Julio Cesar de Souza Francisco<sup>4</sup>, jcesar@utfpr.edu.br**

UTFPR – Universidade Tecnológica Federal do Paraná – Av. Alberto Carazzai, 1640 Cornélio Procópio – PR -86300-000

**Abstract.** Duplex stainless steel samples were aged at low temperatures of the 300 °C and 400 °C for 3000, 5000 and 7000 hours. The changes at the micro-structure were followed during the annealing time using an optical microscopy and measurements of phase percentages. Nano-hardness was used in order to identify the phase responsible for the increasing in the global hardness. The G phase precipitation and  $\alpha'$  phase due to spinodal decomposition was identified by transmission electron microscopy. It was detected that the micro-structural changes affect the global properties, remarkably the global hardness and the corrosion resistance. TEM results showed that the Cr rich precipitation occurs mainly in the ferrite phases. The results also showed a clear difference between the kinetics of precipitation of the lower Cr content sample and the higher Cr sample. The phenomena of precipitation and coalescence of Cr rich phases must be related to the increasing and decreasing tendencies of hardness, respectively and, inversely, the decreasing and increasing tendency of corrosion resistance.

**Keywords:** Spinodal decomposition, Hardness, G phase

## 1. INTRODUCTION

Duplex stainless steels (DSSs) are used in a wide variety of applications, combining good corrosion resistance, weldability and high mechanical strength. The corrosion resistance of these alloys is the same or higher than that of their austenitic analogues and they have higher strength, enabling gauge, weight and cost reductions according to Olsson et al.(2007).

They are little susceptible to stress corrosion cracking and intergranular corrosion, and possess a high pitting corrosion resistance. DSSs have been increasingly used as structural materials in various applications that require high mechanical strength and in highly corrosive environments such as chemical plants, offshore installations, thermal power plants, etc. They are prime candidates for sour well applications where H<sub>2</sub>S, CO<sub>2</sub> and chlorides are found according to (Irissarri,1995), (Massalski,1992) and Shirley et al.(1994).

The properties of DSSs arise from an equilibrium of the austenitic ( $\gamma$ ) and ferritic ( $\alpha$ ) phases obtained by either chemical composition or thermal treatment, and their best properties are achieved with a 50:50  $\alpha/\gamma$  ratio. DSSs are susceptible to the formation of additional phases that can influence their mechanical and corrosion properties according to Zhang et al. (2009).

These phases correspond to the precipitation of various compounds such as chromium carbides, nitrides and several other intermetallic phases (Magnabosco,2009).These phases can be formed during solidification, subsequent heat treatment, or by plastic deformation or aging during their service life according to (Massalski,1992) and Sriram et al.(1989).

As an example, pipes used in primary coolant water in pressurised nuclear reactors are designed for a 40-year service life and their long-term mechanical and corrosion integrity are of the utmost importance for safe operation.

However, aging during service in some temperature ranges can degrade the material's mechanical and corrosion properties according to Yamada et al.(2006) and Shirley et al.(1994). Long-term thermal aging in the range of 300°C – 400°C produces an increase in hardness and tensile properties, together with a decrease in the impact properties, ductility and toughness according to Tavares et al.(2005).

Earlier studies according to (Potgieter,1992) and (Kobayashi,1999) have attributed such degradations of mechanical properties to a spinodal reaction occurring in the ferrite phase, in which the ferrite decomposes into an iron-rich phase and an enriched chromium  $\alpha'$  phase according to Wilms et al.(1994) and Goodwin et al.(1987) , but other precipitated

phases, such as a complex nickel silicide known as G phase, have also been observed and reinforced for Escriba et al.(2009) and (Massalski,1992).

The precipitates occur within the ferrite grain preferentially on dislocations and at  $\alpha$ - $\gamma$  interfaces. It has been reported (Yamada,2006) that G phase precipitation occurs from Cr-rich  $\alpha'$  phase in the second stage of aging, which corresponds to aging of more than 3000 hours at 400 °C.

In the 700°C-1000°C range, increased contents of Cr, Ni and Mo in the steel composition accelerate the precipitation of a  $\sigma$ -phase and other precipitates (nitrides,  $\chi$ -phase), which have a strong negative impact on corrosion resistance according to Chen et al.(2001) and (Potgieter, 1992).

When chromium precipitation occurs, depleted areas cause reductions in the corrosion resistance according to (Miller,1990) and Pumphrey et al.(1990). Moreover, the appearance of the  $\sigma$ -phase is also a ductility-reducing factor according to (Massalski, 1992).

Therefore, despite several studies about the effect of phase precipitation on duplex stainless steel properties according to (Symniotis, 1995) and Sugimoto et al.(1976), there is little information about DSS performance in the presence of precipitation at low temperatures, particularly about its corrosion properties, where an analysis was made of the corrosion properties and passivation of DSS with high chromium content after long-term aging (1000h and 2000 hours) at 300°C and 400°C.

## 2. EXPERIMENTAL PROCEDURES

The samples used in this investigation were obtained from a hot rolled DSS whose composition is given in Tab.1.

Table 1- Composition of the two analysed DSS samples.

Elements	Cr	Ni	C	Mn	Si	P	S	Mo	N
Higher Cr	22,6	5,38	0,024	1,57	0,35	0,013	0,008	2,58	0,13
Lower Cr	17,2	5,37	0,018	1,60	0,037	0,011	0,006	2,54	0,11

However the samples with higher Cr content (22%Cr-5%Ni) were heat treated at 1250°C during 1hour while the samples with lower Cr (17%Cr-5%Ni) content were heat treated at 1300°C during 1hour and quenched in water at 25°C, intending to approximate the ferrite-austenite percentage to 50:50%.

After the solubilization, the samples were aged in a horizontal electric furnace for 3000, 5000 and 7000 hours at two different temperatures (300°C and 400°C) and then quenched in water at 25°C.

The sample structures were visualized using optical microscopy Olympus BX51 and the phases percentages were measured with an image analyser LEICA.

The effect of aging on the corrosion resistance of the alloy under study can probably be ascribed to microstructural changes. To understand these changes, the effect of aging conditions on the hardness of the samples was investigated.

The hardness of the ferrite and austenite of the solubilized and the annealed samples were analyzed using the Nanoindenter XP equipment, with captured images using optical microscopy (Olympus BX51).

All the samples were submitted to an immersion corrosion test during 200h in FeCl<sub>3</sub> solution at 25°C following the ASTM G 38 in aerate environment.

The weight loss after 200h were carefully measured and the results were normalized in function of the exposed area.

Transmission electron microscopy (TEM) was realised in microscope Philips model CM120, and was performed to characterize the annealed samples and identify the changes in the Cr rich phases precipitated during the heat treatment.

Quantitative elemental analysis (WDS) using scanning electron microscopy (SEM) was used in order to quantify the composition of the elements in both ferrite and austenite phases.

## 3. RESULTS

The Fig.1 and Fig.2 following show the TEM micrographs for the annealed samples during 3000h and 7000h mainly at 400°C, to be more representative according to literature, just to verify the precipitation of phases ( $\alpha'$  and G) between the lowest and highest times of treatment in both ferrite and austenite phases.

It is observed that for the lower Cr content sample just one kind of Cr rich precipitate could be detected while for the higher Cr content two kind of Cr rich precipitate could be detected.

Concerning to the size of the precipitates it is plausible to infer that the lower Cr content sample has just G-phase precipitation and the higher Cr content have  $\alpha'$  and G phase precipitation.

However it is known that in the temperature range of 300°C to 600 °C is characterized by the spinodal decomposition of ferrite into Cr-poor  $\alpha$  and Cr-rich  $\alpha'$  domains, which can cause embrittlement of duplex stainless steel alloy.

Other precipitation processes besides  $\alpha'$  phase also occur between 300°C and 600°C in duplex stainless steel, such as G phase precipitation in ferrite and carbide, and  $\gamma_2$  phase precipitation at the grain boundaries. Among these processes, the main one is Ni, Si, Mo-rich G phase precipitation. These particles are very small (1 nm, occasionally up to 50 nm) and are usually present in very high concentrations. They precipitate within the ferrite grain preferentially on dislocations and at  $\alpha$ - $\gamma$  interface.

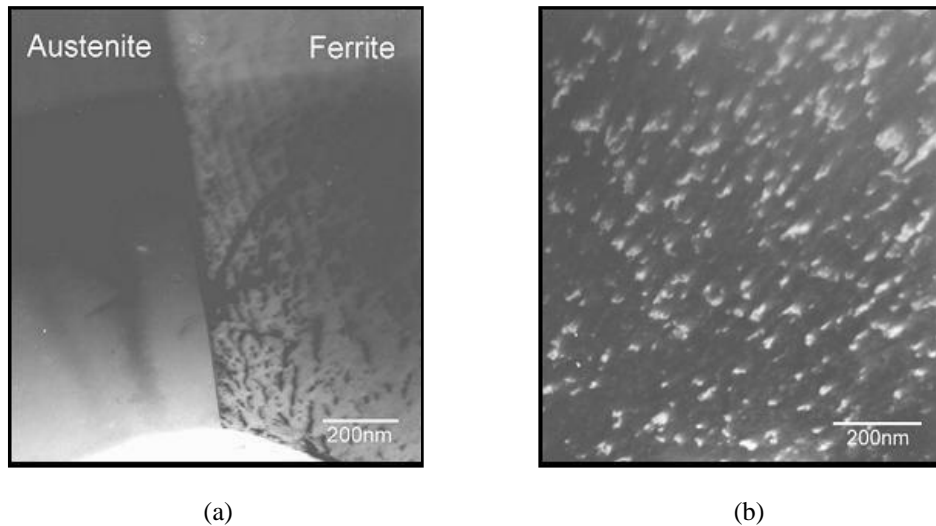


Figure 1: TEM micrograph for the lower Cr content sample annealed at 400°C during: (a) 3000h dark field and (b) G-phase at 7000h bright field.

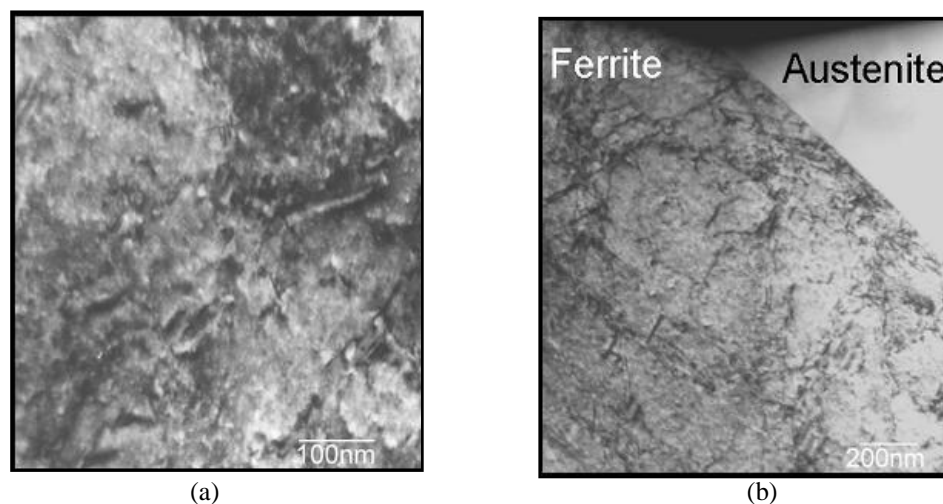


Figure 2: TEM micrograph for the higher Cr content sample annealed at 400°C during: (a) 3000h dark field and (b)  $\alpha'$  and G phase at 7000h bright field.

The Fig.3 shows the ferrite percentage phase for the lower Cr content sample changes of 57% to 30-35% approximately, and the austenite percentage phase increases to 43% to about 65-70%.

But for the higher Cr content sample the ferrite percentage phase increases to 50% to 60% approximately while the austenite percentage phase decreases to 50% to 40%.

The decreasing or increasing tendencies in the phase percentage is related to the original percentage phase of the hot rolled samples.

The lower Cr content sample in the hot rolled condition had 18% of ferrite phase and 82% of austenite phase. The higher Cr content sample had 55% of ferrite phase and 45% of austenite phase in the hot rolled condition.

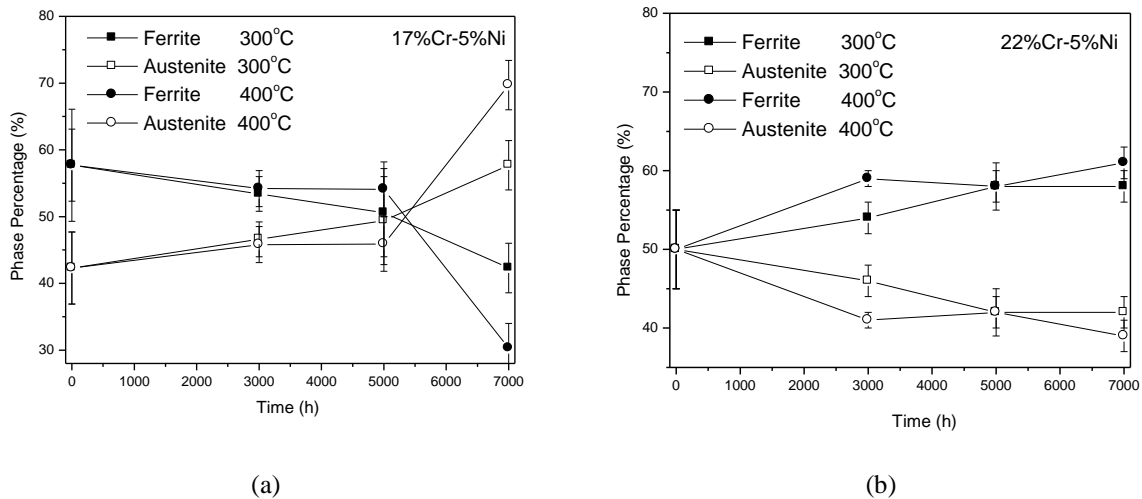


Figure 3: Phases percentage for both samples in function of the annealing time and temperature content (a) lower Cr and (b) higher Cr.

The Fig.4 and Fig.5 show the hardness of the ferrite and austenite phase for the lower and higher Cr content samples, annealed at 300°C and 400°C and the global hardness of the alloy as a function of the aging heat-treatment conditions.

The global hardness represents the average hardness of ferrite and austenite phases.

The effect of aging time on the hardness of austenite was less significant than on that of the ferrite phase and the precipitated phases act as barriers against dislocation motion, resulting in increased global hardness of the alloy.

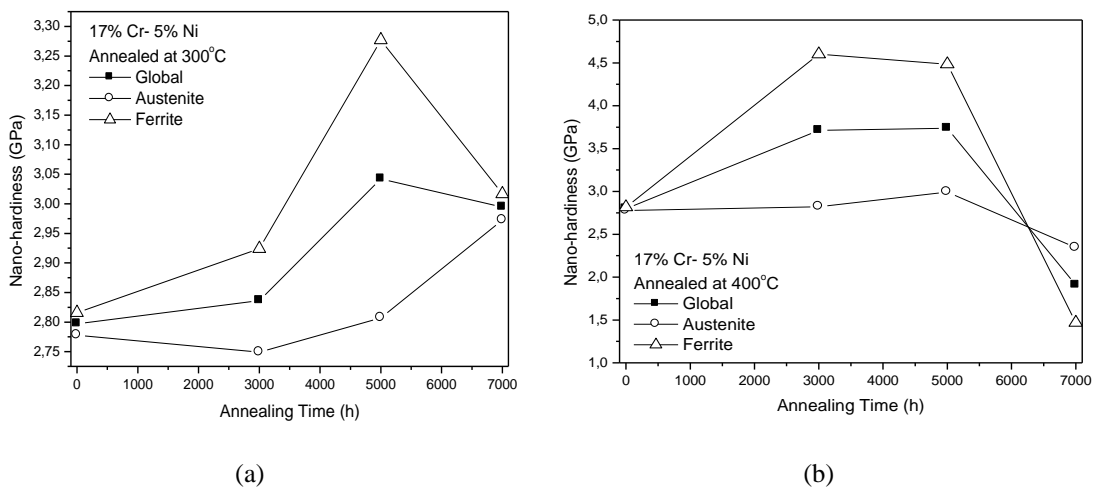


Figure 4: Hardness of the ferrite and austenite phases in function of the annealing time for the lower Cr content samples and annealed at: (a) 300°C and (b) 400°C.

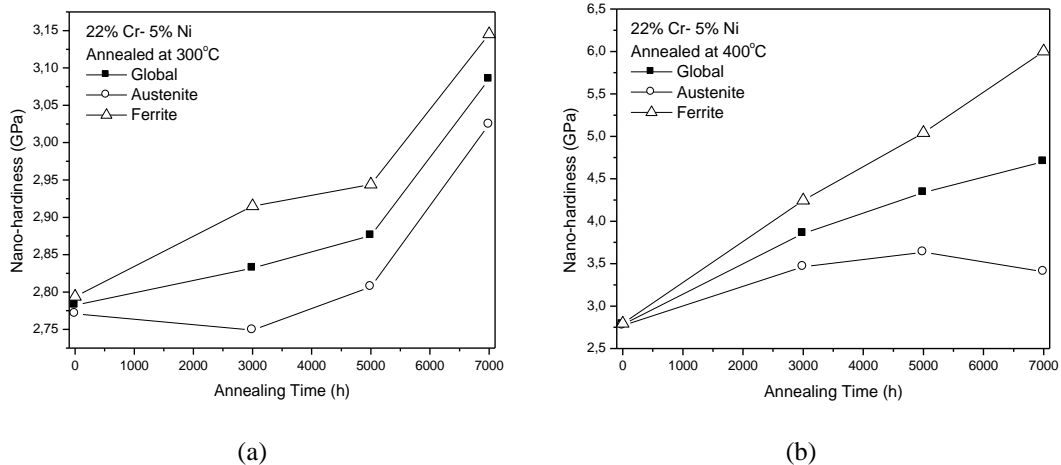


Figure 5: Hardness of the ferrite and austenite phases in function of the annealing time for the higher Cr content samples and annealed at: (a) 300°C and (b) 400°C.

The Tab.2 below shows the contents of the respective elements in austenite and ferrite phases in order to relate these to percentages with their hardness of these phases in isolation.

Table 2: Composition of the ferrite and austenite phases in the samples solubilized higher Cr and lower Cr content.

Elements	Composition (%)			
	22%Cr-5%Ni		17%Cr-5%Ni	
	Austenite	Ferrite	Austenite	Ferrite
Al	0,2322	0,3081	0,0453	0,0552
Si	0,3352	0,3771	0,3257	0,3678
Nb	0,0157	0,0174	0,0292	0,0136
Mo	1,9538	3,0629	2,2133	3,0047
Cr	21,2690	24,8970	16,9732	18,4332
Mn	1,7627	1,5137	1,7435	1,5515
Fe	67,8241	65,6945	72,7838	72,3212
Ni	6,6073	4,1293	5,8859	4,2528

The kinetics of Cr rich precipitation also affects other properties as corrosion. The Fig.6 shows the weight loss in function of the annealing time for the lower and higher Cr content samples.

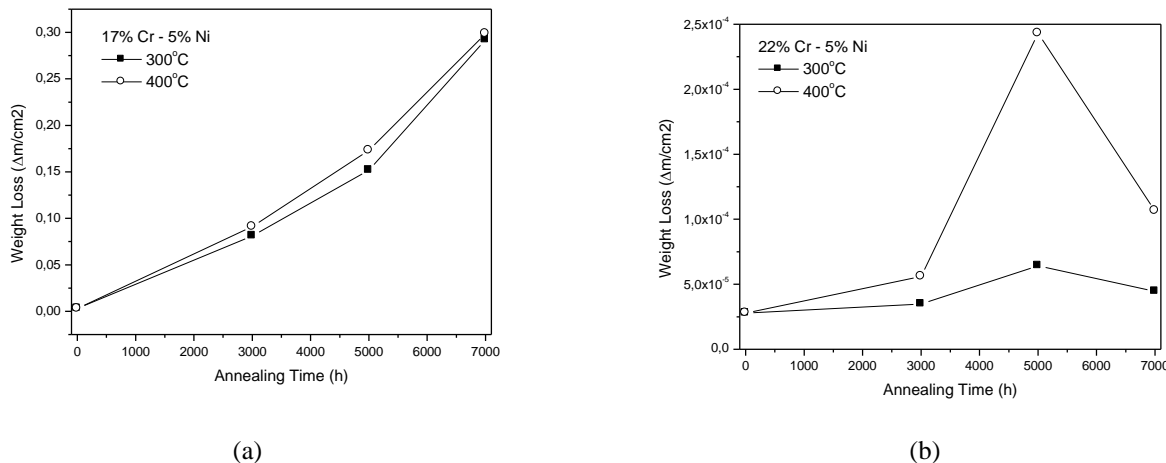


Figure 6 - Weight loss in function of the annealing time for the lower a) and higher b) Cr content. Solution: FeCl<sub>3</sub> 10% for 200h.

The corrosion resistance of the lower and higher Cr content diminishes in function of the annealing time excepted for the higher Cr content annealed at lower temperatures for more than 5000h when it was observed an improvement in the corrosion resistance, confirm that the corrosion rate was highest at an aging time of around 5000 hours.

#### 4. DISCUSSION

The micrographs show an increasing tendency of the ferrite phase percentage for the higher Cr content sample and a decreasing tendency of ferrite phase percentage for the lower Cr content sample. The original hot rolled sample had higher ferrite phase percentage (55%) for the 22%Cr-5%Ni alloy and lower ferrite phase percentage (18%) for the 17%Cr-5%Ni alloy.

The solubilization treatment changed the alloys of their equilibrium state and the annealing slowly took them back to the equilibrium state. For the higher Cr content sample the changes are less evident due to the small percentage of changes.

However for the lower Cr content the percentage of changes is bigger and it is noticeable the new austenite phases presence at the grain boundaries.

The ferrite percentage phase for the lower Cr content sample changes to 57% to 30-35% approximately. The austenite percentage phase increases to 43% to about 65-70%.

For the higher Cr content sample the ferrite percentage phase increases to 50% to 60% approximately while the austenite percentage phase decreases to 50% to 40%. It was visualized that in spite of such macro-structural changes there were micro-structural changes like Cr rich precipitations inside the ferrite grains which contributed to the global hardness increase or decrease and to the corrosion resistance improvement or deployment. The global hardness of the higher Cr content annealed at 300°C continuous increases from 0 to 7000h of annealing time.

However, the increase is more pronounced in the ferrite phase. The TEM showed that the Cr rich precipitation occurs markedly in this phase (probably G-phase). The global hardness of the lower Cr content annealed at 300°C still continuous increases from 0 to 5000h of annealing time but after this time the hardness clearly decrease.

The probable effect associated with this decreasing tendency in the global hardness is the coalescence of the Cr rich phases. TEM showed that just one Cr rich phase was detected in the annealed structure for the lower Cr content and this phase grown up from 3000h to 7000h of annealing time at 400°C. TEM also showed that for the higher Cr content sample there were the presence of two different Cr rich phases (probably  $\alpha'$  and G phases). It was visualized that both phase grown up from 3000h to 7000h at 400°C. The presence of more than one Cr rich phase retards the kinetics of precipitation and the effects were not noticed at 300°C.

The Cr content in the ferrite phase (24%) of the higher Cr content sample is about 30% bigger than the Cr content available in the ferrite phase (18%) of the lower Cr content sample. In the meantime the global hardness for the higher Cr content sample annealed at 400°C stilly showed a decreasing tendency. The lower Cr content sample also showed a decreasing in the global hardness when annealed at 400°C but this tendency starts at 3000h instead of 5000h as mentioned for this same sample annealed at 300°C.

The retarding effect of Cr rich precipitations and the coalescence of these phases must be related with the Cr content. The complete comprehension of these effects is not clearly in the literature, thus it is necessary complementary studies related with these phenomena's.

The corrosion resistance was also affected for these precipitation and coalescence. It was showed that the corrosion resistance was depleted due to the annealing at low temperature but there was a recovering at higher annealing times.

Probably the coalescence results in a rearrangement in the Cr distribution which leads to a more uniform passive film formation and an improvement of the corrosion resistance. This rearrangement must occur manly in the ferrite phase.

The corrosion resistance decreased from 3000h to 7000h as visualized at the immersion results but the sample annealed at 7000h clearly suffered a recover in the corrosion resistance. Additional data are been produced to reinforce this thesis of coalescence and rearrangement of the Cr available.

It is possible that aging manly at 400 °C increases the phase nucleation rate, thus increasing the area of alloy-depleted regions at the precipitate/matrix interface, which justifies the higher rate of corrosion of higher Cr content alloy at 400°C for 5000h of aging.

## 5. CONCLUSIONS

1. The micro-structural changes due to effect of thermal aging affect the global properties remarkably the global hardness and the corrosion resistance, but this effect on the hardness of austenite was less significant than on that of the ferrite phase;
2. The Cr rich precipitation occurs mainly in the ferrite phases;
3. There is a clearly difference between the kinetics of precipitation of the lower Cr content sample and the higher Cr sample but the increase in hardness after 7000 hours of aging indicates that this treatment increased the area per unit volume of the barriers to dislocation motion, probably due the high nucleation rate;
4. The phenomena of precipitation and coalescence of Cr rich phases must be related to the increasing and decreasing tendencies of hardness, respectively and, inversely, the decreasing and increasing tendency of corrosion resistance;
5. A possible increase in corrosion resistance for lower Cr content sample resulting from 7000 hours of aging was related mainly to the diffusion of chromium from the matrix to the chromium-depleted area, which probably did not affect the material's hardness;
6. For higher Cr content sample at 7000 hours of aging the corrosion resistance decreased.

## 6. ACKNOWLEDGEMENTS

UTFPR – Universidade Tecnológica Federal do Paraná - Campus Cornélio Procópio – PR; Prof<sup>o</sup> Dr. Sebastião Elias Kuri and Dr. José Eduardo May of the Laboratory Corrosion - UFSCar – Universidade Federal de São Carlos - Campus São Carlos - SP

## 7. REFERENCES

- Chen, TH and Yang, JR. 2001; Effects of solution treatment and continuous cooling on  $\sigma$ -phase precipitation in a SAF 2205 duplex stainless steel.; *Materials Science and Engineering A.*; 311A pp 28-41.
- Escriba, D. M, Materna-Morris, E, Plaut, RL and Padilha, A. F. 2009; Chi-phase precipitation in a duplex stainless steel.; *Materials Characterization*; V60 pp 1215-1219.
- Ghosh, S.K and Mondal, S. 2008; High temperature ageing behavior of a duplex stainless steel.; *Materials Characterization*. V60 pp 1776-1783.
- Goodwin, S.J. Quayle, B. and Noble, F.W. 1987; *Corrosion.*, Volume 43, n<sup>o</sup> 12, p 743.
- Irissarri, A M. and Erauzkin, E. Sept. 1995 , in Proc. 4<sup>th</sup> European Conf. of Advanced Materials and Processes – Euromat 95; Symposium of Materials and Processing Control - Padua/Venice, Italy, pp. 25-28.
- Kobayashi, D. Y. and Wolyneec, S.; Oct. 1999; *Materials Research*. Volume 2. N<sup>o</sup> 4 S. Carlos, Brazil.
- Magnabosco, R. 2009; Kinetics of sigma phase formation in a duplex stainless steel; *Materials Research*; 12 pp 321-327.
- Massalski , T.B. 1992, *Binary Alloy Phase Diagrams*. ASTM Inter, 2<sup>nd</sup> Ed., p.1771.
- Miller, M.K. and Bentley, J. 1990; *Materials Science and Technology*, Volume 6, p.285.
- NACE Basic Corrosion Course. 1973 4<sup>th</sup> Ed, p.13.
- Olsson, J. and Snis, M. 2007 Duplex – A new generation of stainless steels for desalination plants. *Desalination.*; V205 pp 104-113.
- Potgieter, J.H. 1992; *British Corrosion Journal* , Volume 27, p.219.
- Pumphrey, P.H. and Akhurst, K.N. 1990; *Materials Science and Technology.*, Volume 6, p.211.
- Shirley, D. A.; *Phys. Rev*, 1972, B5, 4770. and Smith, G. C. 1994 ;*Surface Analyses. By Electron Spectroscopy*. Plenum Press.
- Sriram, R. and Tromans, D. 1989; *Corrosion* , Volume 45, N<sup>o</sup> 10 p.809.
- Sugimoto, K and Sawada, Y. 1976; *Corrosion*, Volume 32, N<sup>o</sup> 9 p.347.
- Symniotis, E. 1990; *Corrosion*. Volume 40, p.2.
- Symniotis, E. 1995; *Corrosion Science*, Volume 51, N<sup>o</sup> 8 pp 571 - 580.

- Tavares, S.S.M., Terra, V.F, De Lima Neto, P. and Matos, D.E. 2005; Corrosion resistance evaluation of the UNS31803 duplex stainless steels aged at low temperatures (350 to 550 degrees C) using DLEPR tests. *Journal of Materials Science*; V 40 pp 4025-4028.
- Wilms, M.E., Gadgil, V.J., Krougman, J.M. and Ijsseling, F.P. May 1994; *Corrosion Science*, 1994, Volume 36, Issue 5, , pp. 871-875, 877-881.
- Yamada, T. ; Okano, S. and Kuwano, H. 2006; Mechanical properties and microstructural change by thermal aging of SCS14A cast duplex stainless steel. *Journal of Nuclear Materials* ; V350 pp 47-55.
- Zhang, L. ; Jiang, Y. ; Deng, B. ; Zhang, W. ; Xu, J. and Li, J. 2009; Effect of aging on the corrosion resistance of 2101 lean duplex stainless steel. *Materials Characterization*; V60 pp 1522-1528.

## **8. RESPONSIBILITY NOTICE**

The authors are the only responsible for the printed material included in this paper.